

# Influence of lattice integrity and phase composition on the photocatalytic hydrogen production efficiency of ZnS nanomaterials

## --Supplementary Material

Yangping Hong,<sup>a</sup> Jun Zhang,<sup>b</sup> Xian Wang,<sup>a</sup> Yongjing Wang,<sup>a</sup> Zhang Lin,<sup>a</sup> Jiaguo Yu<sup>\*b</sup> and Feng  
5 Huang<sup>\*a</sup>

*Key Laboratory of Optoelectronic Materials Chemistry and Physics, Fujian Institute of Research on  
the Structure of Matter, Chinese Academy of Sciences, Fuzhou, Fujian, 350002, China*

*State Key Laboratory of Advanced Technology for Material Synthesis and Processing, Wuhan  
University of Technology, Luoshi Road 122#, Wuhan, 430070, P. R. China*

10 \*Corresponding author: [fhuang@fjirsm.ac.cn](mailto:fhuang@fjirsm.ac.cn), [jiaguoyu@yahoo.com](mailto:jiaguoyu@yahoo.com)

### 1. Experimental details.

**The preparation of original ZnS microspheres.** All chemicals were AR reagents from Sinopharm Medicine Company without further purification. The original ZnS microsphere was synthesized by hydrothermal method as reported in our previous work<sup>1</sup>. In details, ZnO (0.167 g, 2 mmol) was  
15 dissolved in a mixture of NaOH (16 M, 12.875 ml) and Na<sub>2</sub>S (1 M, 2 ml) (the final concentration of NaOH solution is 14M after mixing all of them). It was then put into a hydrothermal bomb that was sealed and heated at 230 °C for 12 h. The bomb was forcedly cooled to room temperature rapidly after heat treatment. The white powder was filtered and washed with excess water and absolute ethanol, and finally dried in air at room temperature for 8 h.

20 **The annealing treatments.** The obtained ZnS nanomicrosphere was then annealed for analyzing the effects of different anneal situations on the photocatalytic efficiency of ZnS. For each S ambient annealing treatment, 150 mg ZnS and 100 mg S were put into two little quartz tube respectively, which sealed in a big quartz tube when the vacuum pressure of the tube arrived at 10<sup>-3</sup> Pa, and then annealing at appropriate temperature for certain time in tube furnace.

**Instruments.** X-ray diffraction (XRD) was used to identify the phase composition and average  
25 particle sizes of initial and coarsened samples. Diffraction data were recorded using a PANalytical X'Pert PRO diffractometer with Cu K $\alpha$  radiation (40 kV, 40 mA) in the step scanning mode. The  $2\theta$  scanning range was from 15 to 65° in steps of 0.02° with a collection time of 35 s per step. Scanning electronic microscopy (SEM) analyses were used to confirm the particle size and to determine the particle morphology. Samples were prepared for SEM study by dispersing the ZnS powder onto a  
30 holey carbon-coated support. The SEM analyses were performed using a JSM-6700F instrument.

High-resolution transmission electron microscopy (HRTEM) was used to determine the morphology and detailed microstructure and phase identification of individual particles. Samples were prepared for HRTEM study by dispersing the ZnS powder onto 200-mesh carbon-coated copper grids. HRTEM analyses were performed using a JEOL JEM2010 HRTEM instrument at 200 kV. The nitrogen adsorption and desorption isotherms at 77 K were measured using a Micrometrics ASAP 2020 system after the sample was degassed in vacuum at 120 °C overnight.

**Photocatalytic hydrogen production.** Before photocatalytic experiment, the as-synthesized ZnS needs to be acidized to eliminate the -OH quenching center on the crystal surface<sup>2</sup>. The photocatalytic hydrogen production experiments were performed in a 100 mL Pyrex flask at ambient temperature and 10 atmospheric pressure, and openings of the flasks were sealed with silicone rubber septum. Four low-power UV-LED (3 W, 365 nm) (Shenzhen LAMPLIC Science Co. Ltd. China), which were positioned 1 cm away from the reactor in four different directions, were used as light sources to trigger the photocatalytic reaction. The focused intensity and areas on the flask for each UV-LED were ca. 80.0 mW/cm<sup>2</sup> and 1 cm<sup>2</sup>, respectively. LED appears to be a promising light source for photocatalytic hydrogen production due to its lower energy consumption, high light-emitting efficiency, longer lifetime, cool light without heating and greater durability and reliability. In a typical photocatalytic experiment, 50 mg of catalyst was dispersed with constant stirring in an 80 mL mixed aqueous solution containing 0.1 M Na<sub>2</sub>S and 0.04 M Na<sub>2</sub>SO<sub>3</sub>. Prior to irradiation, the suspension of the catalyst was dispersed in an ultrasonic bath for 5 min, and then bubbled with nitrogen through the reactor for 40 min to completely remove the dissolved oxygen and to ensure the reactor in an anaerobic condition. A 0.4 mL gas was intermittently sampled through the septum, and hydrogen was analyzed by gas chromatograph (GC-14C, Shimadzu, Japan, TCD, nitrogen as a carrier gas and 5 Å molecular sieve column). All glassware was carefully rinsed with distilled water prior to use. The apparent QE was calculated according to Eq. (1):

$$QE[\%] = \frac{\text{number of reacted electrons}}{\text{number of incident photons}} \times 100$$
$$= \frac{\text{number of evolved H}_2 \text{ molecules} \times 2}{\text{number of incident photons}} \times 100 \quad (1)$$

## 2. The calculation of the phase composition and average size of ZnS samples.

Because of the close similarity in the structures of sphalerite and wurtzite, many strong XRD peaks overlap. The phase composition of each sample can be calculated from the integrated intensities of the wurtzite (100) peak ( $2\theta=27.01$ ) and the overlapping sphalerite (111) and wurtzite (002) peaks

( $2\theta=28.64$ ) as illustrated in literature<sup>3</sup>. If the intensity ratio of wurtzite (100) to the overlapping peak is  $R$ , then the weight fraction of wurtzite ( $X_w$ ) can be calculated as

$$X_w = \frac{R}{I_w I_{ws} - R(I_{ws} - 1)} \quad (2)$$

Where  $I_w = 3.88$  represents the intensity ratio of the wurtzite (100) peak to the (002) peak, and  $I_{ws} = 5 = 0.491$  is the intensity ratio of the wurtzite (002) peak to the sphalerite (111) peak.

The decomposition of sphalerite and wurtzite peaks overlapping is fitted by using PersonVII program, as shown in Fig. S1.

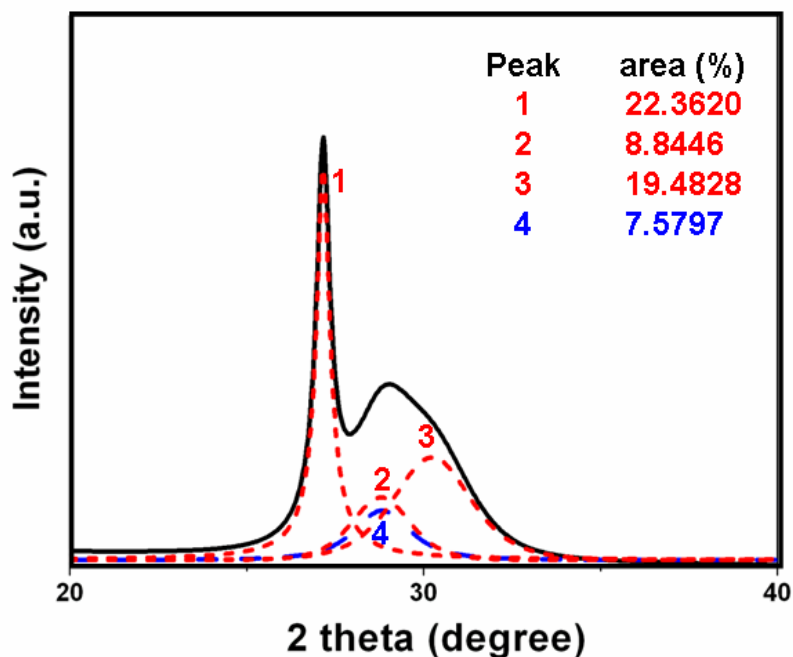


**Fig. S1** The decomposition of the sphalerite and wurtzite peaks overlapping of the original ZnS 10 microsphere. The red refer to the (100), (002) and (101) peaks of the wurtzite and the blue refer to the (111) peak of sphalerite. The wurtzite phase content calculated according to Ref. 4. is 52%.

The average crystallite size was calculated from the peak broadening using the Scherrer equation<sup>4</sup>

$$D = \frac{0.90\lambda}{fwhm \cos \theta} \quad (3)$$

Where  $\lambda$  is the wavelength of Cu  $K\alpha$  radiation (1.5418 Å), 0.90 is the Scherrer constant,  $\theta$  is the Bragg reflection angle, and fwhm is the full width at half-maximum intensity of the chosen XRD peak.

### 3. The difference between vacuum treatment and S ambient treatment.

In order to understand the differences between vacuum treatment and S ambient treatment, we carried out the photocatalytic hydrogen production experiment to the ZnS sample annealed for 3h at 150 °C in vacuum ( $S_{150-3h}^*$ ) (i.e., the sample with the best photocatalytic activity without changing the size, morphology and phase composition). Comparing its hydrogen production rate to that of the 5 sample annealed for 2h at 150 °C in S ambient ( $S_{150-2h}$ ), we found that the former ( $1243 \mu\text{molh}^{-1}\text{g}^{-1}$ ) is greatly less than the latter ( $1723 \mu\text{molh}^{-1}\text{g}^{-1}$ ), which indicates that the S ambient treatment is more beneficial than the vacuum treatment for enhancing the PHPA of samples.

To be specific, due to the high temperature and oxidation protection, the vacuum treatment can promote the regulation of crystal atom lattice unchanging the chemical composition of material, which 10 results in the reduction of main internal lattice defects of ZnS (i.e., twin interfaces and stacking faults<sup>3</sup>). The TEM images in our previous work clearly proved that the lattice integrity enhanced after annealing at 150 °C for 3 h in vacuum<sup>5</sup>. However, the vacuum treatment is hard to eliminate the S atom vacancies (Vs) of ZnS caused by hydrothermal synthesis<sup>6,7</sup>. Thereupon, the S ambient treatment is carried out in this work, not only providing the appropriate temperature for the movement and 15 migration of atoms, but also supplying the S atoms to fill Vs. The lattice integrity thus is improved greatly in S ambient treatment by reducing common defects and Vs.

#### **4. The experiment of photocatalytic degradation eosin B of ZnS samples.**

The experiments of photocatalytic degradation eosin B of  $S_{150-2h}$  and  $S_{150-10h}$  were carried out to further verify the relationship between the photocatalytic activity and phase composition in S ambient. 20 As shown in Fig S2, the absorption peak of  $S_{150-2h}$  is lower than that of  $S_{150-10h}$ , which indicates that the photocatalytic degradation activity of  $S_{150-2h}$  is better than that of  $S_{150-10h}$ . As mentioned above, the size, morphology and surface area of  $S_{150-2h}$  and  $S_{150-10h}$  are similar, the decrease of photodegradation activity is attributed to the variety of wurtzite proportion (52% for  $S_{150-2h}$ , 20% for  $S_{150-10h}$ ). Therefore, it can be concluded that the photocatalytic degradation activity of wurtzite was better than that of 25 sphalerite under similar size. The result of photodegradation eosin B is consistent with that of photocatalytic hydrogen production.

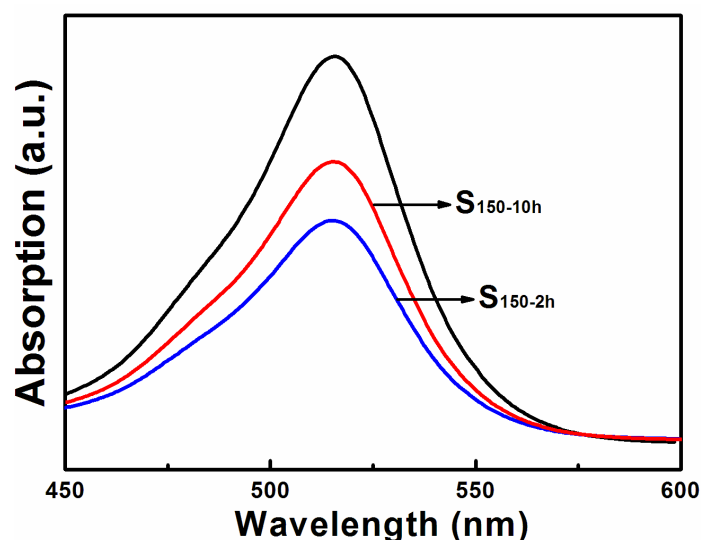


**Fig. S2** The absorption spectra of solutions of eosin B irradiated in the presence of ZnS microsphere (10 mg) annealed at 150 °C for 2 and 10 h in S ambient respectively; the irradiation time is 30 min; the dashed line is the absorption spectrum of the original eosin B solution ( $5.0 \times 10^{-5}$  M, 50 ml).

### 5. The influence of lattice integrity on the photocatalytic activity.

It is generally considered that the photogenerated carriers (electrons and holes) can be easily captured by all forms of defects (lattice internal defects and surface defects), resulting in less diffusion of the photocarriers from the inner to the surface of the material, and further hindering the photocatalytic reaction. The surface defects usually are eliminated by passivating agent<sup>8</sup>, while the internal defects are difficult to be removed. Annealing at the proper temperature may promote the regulation of crystal atom lattice without changing the chemical composition of material, and then may reduce the lattice internal defects.

In ZnS materials, the lattice internal defects, twin interfaces and stacking faults, are formed easily because of the low lattice energy ( $-3319 \text{ kJ/mol}$ )<sup>9</sup>. The reduction of lattice internal defects by annealing the material is beneficial to improve the crystallinity of material, which not only reduces the recombination probability of electron-hole pairs, but also increases the photocatalytic activity.

1. D. S. Li, Z. Lin, G. Q. Ren, J. Zhang, J. S. Zheng and F. Huang, *Cryst. Growth. Des.*, 2008, **8**, 2324-2328.
2. D. S. Li, F. Huang, G. Q. Ren, Z. Y. Zhuang, D. M. Pan and Z. Lin, *J. Nanosci. Nanotechnol.*, 2009, **9**, 6721-6725.
3. F. Huang and J. F. Banfield, *J. Am. Chem. Soc.*, 2005, **127**, 4523-4529.
4. R. Jenkins and R. L. Snyder, *Introduction to X-ray Powder Diffractometry*, John Wiley & Sons, New York, 1996; p 90.
5. Y. P. Hong, Z. Lin, J. Huang, Y. J. Wang and F. Huang, *Nanoscale*, 2011, **3**, 1512-1515.
6. G. D. Watkins, *J Cryst Growth*, 1996, **159**, 338-344.
7. S. Brunner, W. Puff, A. G. Balogh and P. Mascher, *Physica B*, 1999, **273-274**, 898-901.
8. S. F. Wuister, C. de Mello Donegá and A. Meijerink, *J. Am. Chem. Soc.* 2004, **126**, 10397-10402.
9. W. J. Li, E. W. Shi and T. Fukuda, *Cryst. Res. Technol.*, 2003, **38**, 847-858.

